

$B \rightarrow 0$  and  $T = 4.2$  K, in agreement with recent neutron diffractions studies<sup>11</sup> in the same material. This indicates that our pinning centers are rather strong compared to other common defects (dilute arrays of single dislocations or grain boundaries, small precipitates, etc.). We therefore expect the above conclusions to apply also for the majority of other dilute systems. However, the results from our model system do not permit predictions about the behavior of very dense [ $N_v \geq (10a)^{-3}$ ] and/or very strong ( $K_0 > 10^{-10}$  N) pinning centers which sometimes occur in materials with technological applications.

We are grateful to Professor J. R. Clem for a critical reading of the manuscript.

<sup>1</sup>C. P. Bean, Phys. Rev. Lett. **8**, 250 (1962); H. London, Phys. Lett. **6**, 162 (1962).

<sup>2</sup>Y. B. Kim, C. F. Hempstead, and A. R. Strnad,

Phys. Rev. Lett. **9**, 306 (1962).

<sup>3</sup>For a discussion of possible pinning mechanisms see, e.g., A. M. Campbell and J. E. Evetts, Advan. Phys. **21**, 199 (1972); or H. Ullmaier, in *Springer Tracts in Modern Physics* (Springer, Berlin 1975), Vol. 76.

<sup>4</sup>K. Yamafuji and F. Irie, Phys. Lett. **A25**, 387 (1967).

<sup>5</sup>R. Labusch, Cryst. Lattice Defects **1**, 1 (1969).

<sup>6</sup>J. A. Good and E. J. Kramer, Phil. Mag. **22**, 329 (1970).

<sup>7</sup>A. M. Campbell and J. E. Evetts, Advan. Phys. **21**, 199 (1972).

<sup>8</sup>D. Dew-Hughes, Phil. Mag. **30**, 293 (1974).

<sup>9</sup>The metallurgical and superconducting parameters of this system have been investigated in earlier works [G. Antesberger and H. Ullmaier, Phil. Mag. **29**, 1101 (1974); T. Schober and G. Antesberger, Scr. Metall. **7**, 731 (1973)].

<sup>10</sup>H. Ullmaier, Phys. Status Solidi **17**, 631 (1966).

<sup>11</sup>G. Lippmann, in *Proceedings of the International Discussion Meeting on Flux Pinning in Superconductors, St. Andreasberg, Germany, 1974*, edited by P. Haasen (Akademie der Wissenschaften, Göttingen, Germany, 1974).

## Tunneling Conductivity in $4Hb\text{-TaS}_2$

W. J. Wattamaniuk, J. P. Tidman, and R. F. Frindt

*Department of Physics, Simon Fraser University, Burnaby, British Columbia, Canada V5A 1S6*

(Received 1 April 1975)

A  $T^2$  behavior for the conductivity across the layers is observed in  $4Hb\text{-TaS}_2$  crystals below 35 K. This indicates that tunneling occurs between metallic layers separated by an insulating layer. Evidence for thermally activated hopping is observed at higher temperatures.

The superconducting properties of layer compounds intercalated with organic molecules have been explained in terms of superconducting layers coupled via Josephson tunneling.<sup>1</sup> In the normal state in these materials, conduction across the layers should also proceed via tunneling. We present here evidence that quantum mechanical tunneling is the method of conduction across the layers in  $4Hb\text{-TaS}_2$  at low temperatures and that this material may be a prototype for an intercalated system.

In this Letter we present measurements of electrical conductivity as a function of temperature ( $T$ ) for the layered transition-metal dichalcogenide  $4Hb\text{-TaS}_2$ . The change in electrical conductivity across the layers with temperature is explained quantitatively by a model whereby localized charge carriers tunnel quantum me-

chanically from layer to layer, the characteristic signature of a tunneling process being a  $T^2$  dependence of the conductivity at low temperatures. At high temperatures, the small activation energy required to surmount the interlayer barriers dictates that charge transport across the layers proceeds via thermally activated hopping from layer to layer.

The structure of  $4Hb\text{-TaS}_2$  is made up of S-Ta-S molecular layers, stacked  $A, B, C, D, \dots$ .<sup>2</sup> In the  $A$  and  $C$  layers the S atoms surround the Ta in a trigonal-prism coordination; in the  $B$  and  $D$  layers the S atoms surround the Ta in an octahedral coordination. The trigonal-prism coordination occurs in  $2H\text{-TaS}_2$ , which has metallic conductivity along the layers<sup>3</sup> and the octahedral coordination is found in  $1T\text{-TaS}_2$ , which is semiconducting.<sup>4</sup> It has been suggested that  $4Hb\text{-TaS}_2$

can be viewed as a stack of alternating metallic and semiconducting layers, and in fact metallic conductivity is observed along the layers, with evidence for semiconducting behavior perpendicular to the layers.<sup>2</sup>

Tantalum disulfide in powder form, which had been previously reacted from high-purity elements, was transported with iodine vapor in a temperature profile of 720 to 700°C for four weeks, and was then cooled at the rate of 25°/day. The resulting crystals of *4Hb*-TaS<sub>2</sub> were up to 1 mm thick, pyramidal in shape, with shiny flat basal surfaces. The resistivity measurements were made using four-probe techniques both along and across the layers. Contacts were made using a silver colloidal paint. For measurements across the layers ( $\rho_{\perp}$ ) the potential leads were placed on growth steps on the crystal edges as shown in Fig. 1. Resistances were measured to within 1% continuously as a function of temperature over a range 1.2 to 373 K. The values of  $\rho_{\perp}$  are estimated to have an error of about 10%.

Typical resistivity curves for *4Hb*-TaS<sub>2</sub> are shown in Fig. 1. The result for  $\rho_{\parallel}$  (resistivity along the layers) is in agreement with the work of DiSalvo *et al.*<sup>2</sup> and exhibits metallic behavior along the layers. The discontinuities at 21 and 315 K have been attributed to phase transitions

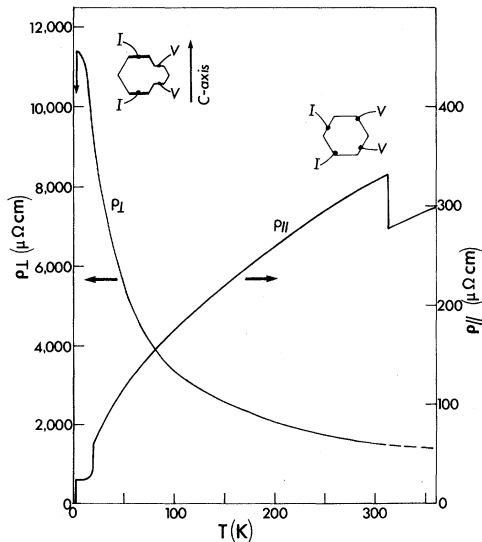


FIG. 1. Resistivity of *4Hb*-TaS<sub>2</sub>. In the dashed region anomalies in  $\rho_{\perp}$  of less than 5% have been observed; however, the behavior is not consistent from sample to sample. In  $\rho_{\parallel}$  the anomalies are centered at 21 and 312 K with thermal hysteresis of 1° and 2°, respectively.

in the charge-density-wave structure in this material.<sup>5</sup> The curve for  $\rho_{\perp}$  in Fig. 1 differs markedly from the results of DiSalvo *et al.*<sup>2</sup> and is the feature of this Letter. Below 315 K,  $\rho_{\perp}$  rises monotonically and reaches a constant value of  $\sim 12000 \mu\Omega \text{ cm}$  at liquid-helium temperatures. At 2.5 K we observe a transition to the superconducting state. For two crystals we have measured both  $\rho_{\perp}$  and  $\rho_{\parallel}$  and obtain results consistent with Fig. 1.

It is important to note that the sharp drop in  $\rho_{\parallel}$  at 21 K is not observed in the measurements of  $\rho_{\perp}$ . This behavior was observed for six out of eight samples measured. The lack of structure in  $\rho_{\perp}$  at 21 K indicates that interlayer shorting is to a large extent absent in the samples. The measured resistivities across the layers at liquid-helium temperatures were all within  $\sim 10\%$  of  $12000 \mu\Omega \text{ cm}$ . The resistivities at 295 K vary up to 50% from sample to sample. These observations suggest that the resistivity behavior at low temperatures is largely intrinsic to the material. We also note that the resistive anomalies observed in the *1T* and *2H* polytypes of TaS<sub>2</sub><sup>4,3</sup> are not present in the data for our *4Hb* crystals, indicating that we have predominantly one polymorph.

We can account for the behavior of the resistivity across the layers for *4Hb*-TaS<sub>2</sub> at low temperatures by using a model in which metallic layers (trigonal-prism-coordination layers) are separated by an insulating gap (octahedral-coordination layers) as shown in Fig. 2. In order to have charge transport at low temperatures, it is necessary for tunneling to occur from one metallic layer to the next. We assume that the charge carriers tunnel through one insulating layer at a time (conserving energy and momentum along the metallic layers) before scattering into thermal equilibrium as determined by the

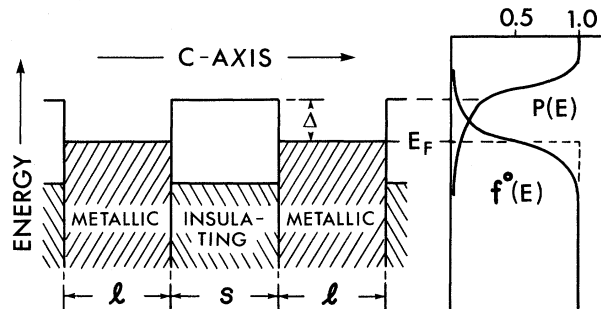


FIG. 2. Multilayer model for *4Hb*-TaS<sub>2</sub>.

local chemical potential. Since tunneling in the low-bias region is Ohmic (the bias voltage across any individual insulating layer is negligibly small relative to the tunneling barrier), we can sum the resistances of the insulating layers assuming that they are all equivalent. The net conductivity across the layers ( $\sigma_{\perp}$ ) is then given by

$$\sigma_{\perp} = (l+s)C, \quad (1)$$

where  $l$  and  $s$  are the dimensions across metallic and insulating layers, respectively, and  $C$  is the conductance per unit area of one insulating layer. The conductance per unit area for a tunnel junction (in the Ohmic region) is given by

Duke<sup>6</sup> as

$$C = \frac{4\pi e^2 m^*}{(2\pi\hbar)^3} \int_0^{\infty} dE \left( -\frac{df^0(E)}{dE} \right) \int_0^E P(E_{\perp}) dE_{\perp}, \quad (2)$$

where  $m^*$  is the effective mass of the carriers within the metallic layers (we assume  $m^*$  to be isotropic) and  $E_{\perp}$  is the kinetic energy associated with carrier motion perpendicular to the layers. The statistical function  $[-df^0(E)/dE]$  limits tunneling to states within thermal energies of the Fermi level of a metallic layer. The term  $\int_0^E P(E_{\perp}) dE_{\perp}$  gives the net tunneling probability for carriers of energy  $E$ . We define  $E_F$  as the Fermi level in the metallic layers and  $\theta^2$  to be the dimensionless constant  $\theta^2 = 2m^*E_F s^2/\hbar^2$ . The conductivity  $\sigma_{\perp}$  can then be expressed as

$$\sigma_{\perp} = 620 \left( \frac{l+s}{s^2} \right) \left\{ \theta^2 \int_0^{\infty} dE \left( -\frac{df^0(E)}{dE} \right) \int_0^E P(E_{\perp}) \frac{dE_{\perp}}{E_F} \right\}, \quad (3)$$

where  $l$  and  $s$  are in angstroms and  $\sigma_{\perp}$  is in reciprocal ohm centimeters.

In the low-temperature region the integral in Eq. (3) may be expanded in the conventional way as a power series in  $T^2$  giving (up to order  $T^2$ )

$$\sigma_{\perp} = 620 \left( \frac{l+s}{s^2} \right) \left\{ \theta^2 \int_0^{E_F} P(E_{\perp}) \frac{dE_{\perp}}{E_F} + \frac{1}{6} \left( \frac{\theta\pi k_B T}{E_F} \right)^2 \left( E_F \frac{dP(E)}{dE} \right)_{E=E_F} \right\}. \quad (4)$$

The zero-temperature conductivity [ given by the first term in Eq. (4) ] will be fairly insensitive to details of the barrier shape. For a square barrier we can approximate the first term by

$$\theta^2 \int_0^{E_F} P(E_{\perp}) dE_{\perp} / E_F \sim 16/\theta^2 \quad (5)$$

provided that the activation energy  $\Delta$  (see Fig. 2) is small ( $\Delta/E_F \ll 1$ ) and  $4 \approx \theta^2$ . The second term in Eq. (4) is proportional to the rate of change of barrier transmission probability with carrier energy and will depend critically on barrier shape. In a system where the Fermi level is in close proximity to the top of the barrier ( $\Delta/E_F \ll 1$ ), the coefficient of  $T^2$  will be significant since it physically indicates the onset of almost perfect transmission as qualitatively illustrated in Fig. 2. The low-temperature conductivity of our model is then given by

$$\sigma_{\perp} = 620 \left( \frac{l+s}{s^2} \right) \left\{ \frac{16}{\theta^2} + \frac{1}{6} \left( \frac{\theta\pi k_B T}{E_F} \right)^2 \left( E_F \frac{dP(E)}{dE} \right)_{E=E_F} \right\}. \quad (6)$$

Equation (6) therefore predicts that  $\sigma_{\perp}$  has a  $T^2$  dependence at low temperatures.

In Fig. 3 we present the experimental data for  $\sigma_{\perp}$  plotted as a function of  $T^2$ . In accordance with our model, the experimental curves are linear below  $\sim 35$  K. The zero-temperature conductivities are within 10% of each other and the slopes of the curves vary from sample to sample. Curves with lower slopes are observed and these can be accounted for within the model by assuming that stacking faults exist in our samples whereby two or more octahedral layers may be situated adjacent to each other (both the slope and the intercept of  $\sigma_{\perp}$  will be decreased, depending on the number of faults). The experimental

conductivity of samples with highest slopes may be expressed as

$$\sigma_{\perp} = 85 + 0.065T^2 \text{ mho/cm}. \quad (7)$$

Below 15 K a deviation from the  $T^2$  curve is observed. It seems plausible that this may in part be related to interlayer shorting, reflecting a rapid increase in conductivity along the layers below the 21-K transition.

An additional feature of our model is the fact that the tunneling conductivity is independent of the density of states in the metallic layers. Therefore changes in the density of states (as suggested by susceptibility measurements<sup>2</sup>) as-

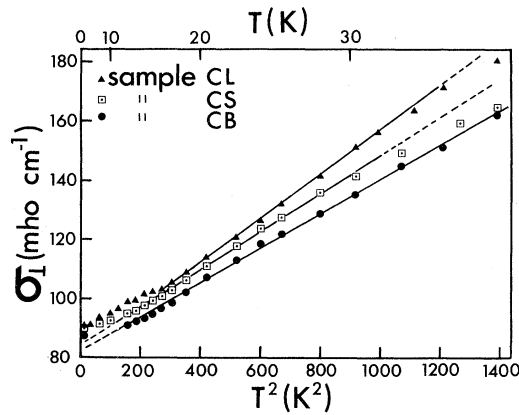


FIG. 3. Measured conductivity across the layers ( $\sigma_{\perp}$ ) as a function of  $T^2$  for a few  $4Hb$ - $TaS_2$  samples.

sociated with the phase transition at 21 K should not be reflected in  $\sigma_{\perp}$ . The absence of any structure in  $\sigma_{\perp}$  at 21 K is strong evidence that the charge-transport mechanism across the layers is independent of the density of states and is in fact the result of tunneling.

Using Eqs. (6) and (7), with  $l = s = 6 \text{ \AA}$ ,<sup>2</sup> and  $E_F = 0.5 \text{ eV}$  (in the absence of any band structure for  $4Hb$ - $TaS_2$  we use the  $E_F$  for  $2H$ - $TaS_2$  from Mattheiss<sup>7</sup>), we obtain the following values for the parameters of our model:  $\theta^2 \sim 40$ ,  $m^*/m_e \sim 8$ , and  $E_F[dP(E)/dE]_{E_F} \sim 160$ , where  $m_e$  is the free electron mass. The low-temperature conductivity is rather insensitive to the magnitude of the activation energy  $\Delta$ . Assuming perfect transmission for energies beyond  $E_F + \Delta$ , the high-temperature conductivity of our model becomes

$$\sigma_{\perp} \approx 620 \left( \frac{l+s}{s^2} \right) \left\{ \frac{16}{\theta^2} + \theta^2 \left( \frac{k_B T}{E_F} \right) \exp\left(-\frac{\Delta}{k_B T}\right) \right\}. \quad (8)$$

The temperature-dependent term is characteristic of an activation or hopping conductivity.

From our measurements above 40 K we obtain estimates for  $\Delta$  of  $\sim 4 \text{ meV}$ .

In conclusion, measurements of  $\sigma_{\perp}$  in  $4Hb$ - $TaS_2$  indicate that conduction perpendicular to the layers takes place via a tunneling process. A simple barrier model gives reasonable qualitative as well as quantitative agreement with the experimental results. The  $T^2$  dependence of  $\sigma_{\perp}$  at low temperatures is perhaps the strongest indication of the presence of a tunneling process in our samples.

Details of the model calculations and further work will be the subject of a more comprehensive paper.

We are grateful to the National Research Council of Canada for financial assistance. We acknowledge the many conversations we have had with T. M. Rice and the technical assistance of G. A. Scholz.

<sup>1</sup>W. Lawrence and S. Doniach, in *Proceedings of the Twelfth International Conference on Low Temperature Physics, Kyoto, 1970*, edited by E. Kanda (Keigaku Publishing Co., Kyoto, 1971), p. 361.

<sup>2</sup>F. J. DiSalvo, B. G. Bagley, J. M. Voorhoeve, and J. V. Waszczak, *J. Phys. Chem. Solids* **34**, 1357 (1973).

<sup>3</sup>J. P. Tidman, O. Singh, A. E. Curzon, and R. F. Frindt, *Phil. Mag.* **30**, 1191 (1974).

<sup>4</sup>A. H. Thompson, F. R. Gamble, and J. F. Revelli, *Solid State Commun.* **9**, 981 (1971).

<sup>5</sup>J. A. Wilson, F. J. DiSalvo, and S. Mahajan, *Advan. Phys.* **24**, 117 (1975).

<sup>6</sup>C. B. Duke, *Tunneling in Solids*, Suppl. No. 10 to *Solid State Physics*, edited by H. Ehrenreich, F. Seitz, and D. Turnbull (Academic, New York, 1969), pp. 49-65.

<sup>7</sup>L. F. Mattheiss, *Phys. Rev. B* **8**, 3719 (1973).